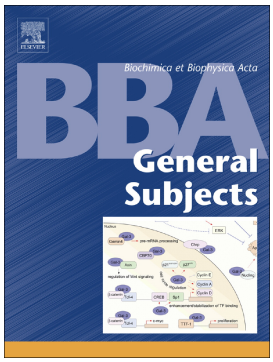

Identification of amino acid residues critical for the B cell growth-promoting activity of HIV-1 matrix protein p17 variants

Wangxiao He, Pietro Mazzuca, Weirong Yuan, Kristen Varney, Antonella Bugatti, Alfredo Cagnotto, Cinzia Giagulli, Marco Rusnati, Stefania Marsico, Luisa Diomede, Mario Salmona, Arnaldo Caruso, Wuyuan Lu, Francesca Caccuri

PII: S0304-4165(18)30304-0
DOI: doi:10.1016/j.bbagen.2018.09.016
Reference: BBAGEN 29219

To appear in: *BBA - General Subjects*

Received date: 9 July 2018
Revised date: 18 September 2018
Accepted date: 19 September 2018

Please cite this article as: Wangxiao He, Pietro Mazzuca, Weirong Yuan, Kristen Varney, Antonella Bugatti, Alfredo Cagnotto, Cinzia Giagulli, Marco Rusnati, Stefania Marsico, Luisa Diomede, Mario Salmona, Arnaldo Caruso, Wuyuan Lu, Francesca Caccuri , Identification of amino acid residues critical for the B cell growth-promoting activity of HIV-1 matrix protein p17 variants. Bbagen (2018), doi:10.1016/j.bbagen.2018.09.016

Identification of amino acid residues critical for the B cell growth-promoting activity of HIV-1 matrix protein p17 variants

Wangxiao He,[a] Pietro Mazzuca,[b] Weirong Yuan,[c] Kristen Varney,[d] Antonella Bugatti,[b] Alfredo Cagnotto,[e] Cinzia Giagulli,[b] Marco Rusnati,[b] Stefania Marsico,[f] Luisa Diomede,[e] Mario Salmona,[e] Arnaldo Caruso,[b] Wuyuan Lu,[a,c,d] Francesca Caccuri,[b*]

[a]Center for Translational Medicine, Xi'an Jiaotong University School of Life Science and Technology, Xi'an, China; [b]Department of Molecular and Translational Medicine, University of Brescia Medical School, Brescia, Italy; [c]Institute of Human Virology, University of Maryland School of Medicine, Baltimore, USA; [d]Department of Biochemistry and Molecular Biology, University of Maryland School of Medicine, Baltimore, USA; [e]IRCCS Istituto Ricerche Farmacologiche "Mario Negri" Milan, Italy; [f]Department of Pharmacy,Health and Nutritional Sciences, University of Calabria, Arcavacata di Rende, Italy.

[*]Corresponding author at: Department of Molecular and Translational Medicine, Section of Microbiology and Virology, University of Brescia Medical School, Brescia, Piazzale Spedali Civili, 1 – 25123 Brescia, Italy.

E-mail addresses: hewangxiao5366@sina.com (W. He), p.mazzuca@unibs.it (P. Mazzuca), wyuan@ihv.umaryland.edu (W. Yuan), kvarney@som.umaryland.edu (K. Varney), antonella.bugatti@unibs.it (A. Bugatti), alfredo.cagnotto@marionegri.it (A. Cagnotto), cinzia.giagulli@unibs.it (C. Giagulli), marco.rusnati@unibs.it (M. Rusnati), stefania.marsico@unical.it (S. Marsico), luisa.diomede@marionegri.it (L. Diomede), mario.salmona@marionegri.it (M. Salmona), arnaldo.caruso@unibs.it (A. Caruso), wlu@ihv.umaryland.edu (W. Lu), francesca.caccuri@unibs.it (F. Caccuri).

Running Title: The p17 epitope for B cell proliferation.

Key words: HIV-1; matrix protein p17; p17 variants; p17 clonogenic epitope; B cell proliferation; lymphoma.

Abbreviations: HIV-1, human immunodeficiency virus type 1; AIDS, acquired immunodeficiency syndrome; cART, combined antiretroviral therapy; NHL, non-Hodgkin's lymphoma; CD, circular dichroism; NMR, nuclear magnetic resonance; SPR, surface plasmon resonance; CXCR, chemokine (C-X-C motif) receptor; LN-LEC, lymph node derived lymphatic endothelial cell; PI3K, phosphatidylinositol 3-kinase; ERK, extracellular signal-regulated kinase; MEK, mitogen-activated protein kinase kinase.

Abstract

Background: HIV-1 matrix protein p17 variants (vp17s) detected in HIV-1-infected patients with non-Hodgkin's lymphoma (HIV-NHL) display, differently from the wild-type protein (refp17), B cell growth-promoting activity. Biophysical analysis revealed that vp17s are destabilized as compared to refp17, motivating us to explore structure-function relationships. *Methods*: We used: biophysical techniques (circular dichroism (CD), nuclear magnetic resonance (NMR) and thermal/GuHCL denaturation) to study protein conformation and stability; Surface plasmon resonance (SPR) to study interactions; Western blot to investigate signaling pathways; and Colony Formation and Soft Agar assays to study B cell proliferation and clonogenicity. *Results*: By forcing the formation of a disulfide bridge between Cys residues at positions 57 and 87 we obtained a destabilized p17 capable of promoting B cell proliferation. This finding prompted us to dissect refp17 to identify the functional epitope. A synthetic peptide (F1) spanning from amino acid (aa) 2 to 21 was found to activate Akt and promote B cell proliferation and clonogenicity. Three positively charged aa (Arg15, Lys18 and Arg20) proved critical for sustaining the proliferative activity of both F1 and HIV-NHL-derived vp17s. Lack of any interaction of F1 with the known refp17 receptors suggests an alternate one involved in cell proliferation. *Conclusions*: the molecular reasons for the proliferative activity of vp17s, compared to refp17, relies on the exposure of a functional epitope capable of activating Akt. *General significance*: Our findings pave the way for identifying the receptor(s) responsible for B cell proliferation and offer new opportunities to identify novel treatment strategies in combating HIV-related NHL.

1. Introduction

Combined antiretroviral therapy (cART) for human immunodeficiency virus type 1 (HIV-1) dramatically reduces viral load and slows disease progression, contributing to a steady decline in AIDS-related mortality among HIV-1 seropositive (HIV^+) individuals. cART has also changed the leading cause of mortality in HIV^+ patients from opportunistic infections (in the pre-cART era) to malignancies (in the cART era), with the latter accounting for roughly one-third of all AIDS and non-AIDS-related deaths today [1]. While AIDS-defining malignancies as Kaposi sarcoma (KS), non-Hodgkin's lymphoma (NHL) and cervical cancer have significantly decreased since the introduction of cART, non-AIDS-defining malignancies such as lung and anal cancers and Hodgkin's lymphoma (HL) have seen a rapid increase during the same period of time [2, 3]. Nevertheless, NHL still remains persistently elevated in people living with HIV/AIDS and the leading cause of death in these patients [2]. Considering the prolonged survival granted by cART, an increasing number of malignant lymphomas are expected to occur in these patients in the next decade. Understanding the molecular mechanisms underlying HIV-1-associated lymphomagenesis is important for both diagnostic and therapeutic interventions of these aggressive cancers.

A possible direct role of HIV-1 and its gene products in lymphomagenesis has been seldom considered being its genome not detectable in the malignant B cells. For this reason, different mechanisms have been invoked for the initial transformation of B cells, notably Epstein-Barr virus (EBV) and Kaposi's Sarcoma herpesvirus (KSHV) infections [4, 5] and HIV-1-triggered immune dysfunction [6]. However, several recent lines of evidence suggest that a HIV-1 structural protein, namely the matrix protein p17 (p17), may be functionally linked to HIV-1-associated lymphomagenesis. First, despite being a protein essential for viral assembly and maturation [7], biologically active p17 is actively secreted from HIV-1-infected cells [8], and can be detected in blood [9] and in lymph node germinal centers of HIV^+ individuals, where it

persists long after cART suppression of HIV-1 [10]. Second, high levels of p17, but not of other viral proteins, are found in lymph nodes of HIV-1 transgenic mice with early-stage lymphoma [11]. Third, p17 promotes receptor-mediated angiogenesis and lymphangiogenesis of vascular and lymphatic endothelial cells *in vitro* and *in vivo* [12-14]. Fourth, p17 deregulates the biological activity of immune cell populations relevant in the context of AIDS pathogenesis [15] after interaction with heparan-sulphate proteoglycans [16] and with two chemokine receptors, namely CXCR1 and CXCR2, expressed on target cells [12, 17].

HIV-1 associated lymphoma correlates with viral replication [18] where p17 is extremely prone to mutate [19]. We have recently demonstrated that p17 variants (vp17s) isolated from the NHL specimens (both blood and tissue) of HIV^+ patients promote B cell growth by activating the pro-survival and oncogenic Akt signaling pathway [20]. Two categories of NHL-derived vp17s that promote B cell growth and activate the Akt pathway have been identified: the first shows amino acid (aa) insertions at position 117-118 and the second is characterized by aa insertions at position 125-126. Ultra-deep pyrosequencing (UDP) showed that these two categories of vp17s are more frequently detected in plasma of HIV^+ subjects with than without NHL [20]. Mutational analysis of these natural vp17s has led us to hypothesize that the B cell growth-promoting activity is conferred on certain vp17s with destabilized protein structure and/or possibly altered protein conformation [20]. The work reported here aims to gain mechanistic insight into the role of vp17s in B cell proliferation by integrating functional analysis and receptor binding.

2. Materials and methods

2.1. Reagents

Synthetic phospholipid blend [Dioleoyl] DOPC:DOPS [7:3 w/w] was purchased from Avanti Polar Lipids (Alabaster). Detergent CHAPS and cholesteryl hemisuccinate tris salt (CHS) were from Sigma-Aldrich. Research-grade CM5 sensorchips, 1-ethyl-3-(3-diaminopropyl)-carbodiimide hydrocloride (EDC), N-hydroxysuccinimide (NHS) and the anti-GST antibody were from GE-healthcare. Human recombinant CXCR1 and CXCR2 fused to a glutathione S-transferase (GST-CXCR1 and GST-CXCR2) was from Abnova. Conventional heparin (13.6 kDa) was obtained from a commercial batch preparation of unfractionated sodium heparin from beef mucosa (Laboratori Derivati Organici S.p.A.) purified (up to 95%) from contaminants according to described methodologies.

2.2. Recombinant and synthetic HIV-1 refp17 proteins and mAbs to p17

Recombinant proteins (in their monomeric form) were purified (> 98%) by reverse-phase fast performance liquid chromatography as previously described [21]. The absence of endotoxin (LPS) contamination (< 0.25 endotoxin units per ml) in protein preparation was assessed by Limulus amoebocyte assay (Associates of Cape Cod Inc.). Synthetic refp17 was obtained as previously described [22]. P17 mAb MBS-3 was produced and purified in our laboratory as previously described [21].

2.3. Cell cultures

Human lymphoma B cell lines Raji and BJAB were cultured in RPMI 1640 containing 10% (vol/vol) fetal bovine serum (FBS). Jurkat T leukemic cell line was cultured in RPMI

1640 (Sigma) supplemented with 10% fetal bovine serum (FBS) (Sigma) and 2 mM L-glutamine (Sigma) (complete medium). Lymph nodes derived lymphatic endothelial cells (LN-LECs) were isolated and characterized as previously described [23] and cultured in endothelial growth medium (EGM) (Lonza) containing 10% (vol/vol) FBS and supplemented with VEGF-C (0.025 µg/ml; Reliatech). All experiments were carried out with cells at passages 2–6.

2.4. Viable cell counting

Propidium Iodide (PI) staining (Immunostep) was used to detect PI^- viable cells by flow cytometry. Absolute cell counts were obtained by the counting function of the MACSQuant® Analyzer (Miltenyi Biotec).

2.5. CD Spectroscopy and Thermal/GuHCL Denaturation

CD spectra of p17 proteins at a concentration of 2.5 µM in 10 mM phosphate buffer (PBS) (pH 7.4) were obtained at room temperature on a J-810 spectropolorimeter (Jasco, Easton, MD) using a 1-mm quartz cuvette. Protein thermal denaturation was carried out in PBS on the JASCO CD spectrometer equipped with a temperature controller. 2.5 mL of protein solution (10 µM) prepared in PBS, pH 7.4, was aliquoted into a 3-mL cuvette. Under constant stirring, measurements were taken at a one-degree interval between 25 and 90 °C, at a heating rate of 1 °C per minute. After each 1-minute heating cycle and a 20 s wait time, CD signals at 222 nm were sampled over a 16-s period. Heating and data acquisition were fully automated with the control software provided by JASCO. GuHCl-induced protein denaturation monitored by CD spectroscopy at 222 nm was carried out at room temperature. Specifically, an initial 3.0 mL of protein solution prepared at 10 µM in 10 mM phosphate

buffer (pH 7.2) was aliquoted into a 10-mm cuvette. An increasing amount of aliquot was withdrawn, followed immediately by addition of an equal volume of denatured protein of the same concentration, prepared in 10 mM phosphate buffer containing 8 M GuHCl (pH 7.2). This procedure generated a stepwise increase (0.25 M/step) in the concentration of GuHCl in the cuvette from 0 to 4 M after 16 withdrawal/addition cycles. The solution in the cuvette was thoroughly mixed before signals at 222 nm were recorded at different GuHCl concentrations. The experimental data from thermal and chemical denaturation were subjected to a six-parameter nonlinear regression analysis as described previously [20, 21].

2.6. Dynamic light scattering

Concentrated protein solutions were filtered using a Whatman Anotop 10 filter (0.22 mm) and, after UV quantification, diluted in PBS to a final concentration of 10 mM each. Protein size measurements were carried out at 25 °C, pH 7.4, with a total ionic strength of 0.1 M, on a Malvern Zetasizer Nano ZS instrument. Twenty runs of 30 s each were taken and averaged, and the data were processed using the manufacturer provided software.

2.7. NMR spectroscopy

NMR spectra were recorded at 25 °C on an 800 MHz (800.27 MHz for protons) Bruker Avance-series NMR spectrometer equipped with four frequency channels and a 5 mm triple-resonance z-axis gradient cryogenic probehead. A one-second relaxation delay was used and quadrature detection in the indirect dimensions was obtained with states-TPPI phase cycling; initial delays in the indirect dimensions were set to give zero- and first-order phase corrections of 90° and –180°, respectively [25, 26]. Data were processed using the processing program nmrPipe on Mac OS X workstations [27]. 2D NOESY experiments with a 150 ms

mixing time were collected to monitor changes in the backbone and side-chain 1H protein resonances [28]. Typical NMR samples contained 3 mg/ml protein in a 10 mM sodium phosphate and 25 mM sodium chloride buffer (pH 7.4) to which 10% D2O (v/v) was added.

2.8. Soft agar

Anchorage-Independent Growth Assay. Raji (12,500 cells/well) and BJAB (2,000 cells/well) cells were plated in 12-well plates in 2 ml RPMI containing 5% FBS and 0.35% and 0.5% Sea-Plaque agarose (Lonza), respectively, over a 0.7% agarose base. One day after plating, medium containing treatments, as indicated, was added to the top of the layer and replaced every 4 d. After 10 d, 300 µl of MTT (Sigma-Aldrich) were added to each well and allowed to incubate for 4 h at 37 °C. Plates were then placed overnight at 4 °C, and colonies > 50 µm in diameter were counted.

2.9. B cell colony formation assay

Raji cell suspension was sequentially diluted, and cells were seeded by manual pipetting into a 96-well plate at a dilution of 0.5 cells/well. Plates were incubated for 8 d under standard conditions (RPMI medium supplemented with 10% FBS) in the presence or absence of 0.01 µg/ml of Peptide F1. When reported, Peptide F1 was pre-incubated for 30 min at 37 °C with 1 µg/ml of unrelated control mAb (Ctrl mAb) or p17 neutralizing mAb MBS-3. In selected experiments, Raji cells were cultured with Peptide F1 in the presence or absence of inhibitors of PI3K/Akt (Akt VIII i) (1 µM) (Sigma-Aldrich) or mitogen-activated protein kinase (MEK)/ERK1/2 (PD98059) (10 µM) (Calbiochem) signaling pathways. Eight days after culture plates were analyzed for single colony formation.

2.10. Western blot analysis

Raji cells were starved for 24 h by serum deprivation (RPMI containing 1mM L-glutamine and 0.5% FBS). Cells (7 x 10^5/ml) were treated with different concentrations of Peptide F1 and lysed in 200 µl of of 10 mM Hepes (pH 7.9), 10 mM KCl, 1.5 mM MgCl2, 0.5 mM EGTA, 0.5 mM EDTA, and 0.6% Nonidet P-40, containing a mixture of protease inhibitors (Complete Mini Roche) and phosphatase inhibitors (sodium vanadate, PAO, and sodium fluoride). Equal amounts of total protein were resolved on a 12% SDS-polyacrylamide gel and then electroblotted onto a nitrocellulose membrane. The blots were incubated overnight at 4 °C with the following rabbit primary monoclonal antibodies to pAkt (Ser473), total Akt, pERK1/2 (Thr202/Tyr204) or total ERK1/2 (all purchased from Cell Signaling Technology). The antigen-antibody complex was detected by incubation of the membranes for 1 h at room temperature with peroxidase-coupled goat anti-rabbit IgG (Thermo Scientific) and revealed using the ECL System.

2.11. *In vitro* tube formation assay

Pre-chilled 48-well culture plates were coated with 150 µl per well of basement membrane extract (BME) (10 mg/ml) (Cultrex; Trevigen) and incubated for 30 min at 37 °C. LN-LECs were nutrient starved for 24 h in endothelial basal medium (EBM) containing 0.5% FBS and then harvested and resuspended in EGM supplemented with 10% FBS. Cells were seeded in the BME-coated plate (5×10^4 per well) and treated or not with 0.01 µg/ml of refp17, SS-p17, NHL-a101 or NHL-a102.

2.12. SPR binding assay

SPR measurements were performed on a BIAcore X-100 instrument (GE-Healthcare). For the analysis of the interaction of p17-derived peptides with CXCR1 and CXCR2, anti-GST antibodies (catalog#G7781) (Sigma-Aldrich) were immobilized onto a CM5 sensorchip (GE Healthcare) using standard amine-coupling chemistry. Then, recombinant human

CXCR1 and CXCR2 with a C-terminal GST tag [10 µg/ml in 50 mM HEPES pH 7.0 containing 0.01% CHS, 0.1% CHAPS and 0.33 mM synthetic phospholipid blend (dioleoyl) DOPC:DOPS (7:3 w/w), (running buffer)] were injected over the anti-GST surface, allowing the immobilization of 830 and 290 resonance units (RU) respectively (equal to 12.7 and 4.5 fmoles/mm^2, respectively). A sensorchip coated with anti-GST antibodies was used as a negative control and for blank subtraction. For the analysis of the interaction of p17-derived peptides with heparin, the latter was biotinylated at its reducing end and immobilized onto a SA sensorchip containing pre-immobilized streptavidin (GE Healthcare), allowing the immobilization of 280 RU, equal to 20.5 fmoles/mm^2 of heparin. The screening of the capacities of the various p17-derived peptides to bind p17 receptors was performed in single cycle analysis as follows: the peptides were resuspended at a final concentration of 20 µM in running buffer (for analysis on CXCR1 and CXCR2) or in HBS-EP+ (for analysis on heparin), injected over the different surfaces for 2 min (CXCR1, CXCR2 and control anti-GST antibody surfaces) or for 4 min (heparin and control streptavidin surfaces) and then washed until dissociation.

2.13. Statistical analysis

Data were analyzed for statistical significance using Student's t-test or one-way ANOVA. Bonferroni's post-test was used to compare data. Differences were considered significant at $P < 0.05$. Statistical tests were performed using GraphPad Prism 5 software (GraphPad).

3. Results

3.1. p17 has an intrinsic ability to promote B cell growth

Previous results showed that mutation-induced p17 destabilization may lead to a conformational change responsible for the viral protein to promote B cell proliferation, thus supporting the hypothesis that such activity is intrinsic to the p17 molecule itself [20, 29]. The p17 protein of 132 amino acid residues comprises five α-helices connected primarily by short loops (Fig. 1A) [29-31]. P17 contains two conserved Cys residues at positions 57 and 87, whose two buried sulfur atoms are 9.7 Å apart in the native structure [32] too far to form a disulfide bridge (Fig. 1B). A forced formation of the disulfide bridge is expected to drastically alter p17 conformation and destabilize the protein (SS-p17) to such an extent that its activity on B cell growth may be seriously affected. In order to test this hypothesis, we first chemically synthesized large quantities of highly pure (2-132) p17 [23], whose sequence was derived from the HIV-1 clade B isolate BH10 (UniProtKB P04585; refp17) and compared the amide-amide NOESY NMR spectra of synthetic with recombinant refp17 protein [22] collected at 25 ºC, pH 7.4. The broadly dispersed NOE signals are characteristic of well-folded helical proteins; the NOE signals of both proteins are largely overlapping, suggesting they are structurally highly similar in solution, if not identical (Fig. 1C). We compared both proteins in a transformed B cell colony formation assay and, as shown in Fig. 1D, synthetic and recombinant refp17 displayed similar activities in inhibiting the growth of Raji cells. These results demonstrate that the synthetic refp17 protein is indeed correctly folded and fully functional.

Then, we prepared oxidized SS-p17 by dissolving synthetic refp17 at a concentration of 0.1 mg/ml in PBS containing 10% DMSO and 2 M Guanidinium chloride (GuHCl), pH 7.4, and continuing the oxidation reaction under partially denaturing conditions for 12 h at room temperature. Oxidative formation of disulfide bonds in a peptide or protein can be

achieved by using the oxidizing reagent DMSO [33, 34, 35]. The oxidation product, SS-p17, was verified by ESI-MS and purified to homogeneity by RP-HPLC. Analysis of synthetic refp17 and SS-p17 by circular dichroism (CD) spectroscopy (Fig. 2A) indicated that while synthetic refp17 adopted an α-helical conformation characterized by two negative peaks at 208 and 222 nm and one strong positive peak at 195 nm, consistent with known structural features of refp17 [32, 36], SS-p17 displayed a drastically reduced α-helicity at room temperature. When temperature was raised from 25 to 37 ºC, α-helicity further decreased with a more pronounced effect on SS-p17 than on refp17. These data suggest that forced disulfide bonding in refp17 causes the protein to partially unfold. Partial unfolding of refp17 necessarily destabilizes the protein. We quantified protein stability by subjecting synthetic refp17 and SS-p17 to GuHCl-induced chemical denaturation a process monitored by CD spectroscopy at 222 nm. As shown in Fig. 2B, both proteins progressively lost structure at 25 ºC as concentration of the chemical denaturant increased, with refp17 being significantly more stable than SS-p17. A non-linear regression analysis based on a two-state, single transition model gave rise to free energy changes, ΔG, associated with protein denaturation of 6.4 and 3.0 kcal/mol for refp17 and SS-p17, respectively. These results indicate that over half of the stabilization energy for p17 was lost as a result of disulphide bonding. Heat-induced protein thermal denaturation monitored at 222 nm by CD spectroscopy corroborated these findings. As shown in Fig. 2C, refp17 exhibited a co-operative unfolding with a single transition as temperature was raised from 25 °C to 90 °C, typical of a compact, single-domain globular protein. Normalization of the experimental data based on a two-state protein denaturation model gave rise to a characteristic melting temperature (Tm at which 50% of protein is denatured or unfolded) of 60.8 °C for refp17. By sharp contrast, disulfide bonding dramatically destabilized refp17 by more than 17 °C (Tm = 43.4 °C). To further evaluate the effect of disulfide bonding on refp17 structure, we analysed both proteins using NOESY NMR spectroscopy. The aliphatic-aliphatic (Fig. 2D) and amide-amide (Fig. 2E) NOEs of SS-

p17 are markedly less abundant than those of refp17, suggesting that the former is substantially less structured than the latter. Since formation of soluble aggregates of a protein can also contribute to dampened NOE signals, we used dynamic light scattering techniques to analyse the tendency of refp17 to oligomerize/multimerize in solution at room temperature. As shown in Fig. 2F, the particle radii of refp17 and SS-p17 were measured to be 2.4 and 18 nm, respectively. These results indicate that while refp17 existed as a monomer in solution, SS-p17 formed an oligomer/multimer. The strong tendency of SS-p17 to oligomerize/multimerize at high concentrations in solution was indicative of a disulfide-bonding-induced exposure of some buried hydrophobic residues. Taken together, our extensive biochemical and biophysical data demonstrate that disulfide bonding between Cys57 and Cys87 significantly altered refp17 structure and destabilized the viral protein. We therefore tested the B cell growth-promoting activity of SS-p17 on Raji cells in an anchorage independent colony formation assay. As shown in Fig. 2G, refp17 as expected inhibited the growth of Raji and BJAB cells whereas SS-p17 significantly promoted colony formation.

3.2. The pro-lymphangiogenic activity of refp17 is independent of protein structure and stability

Refp17 is capable of promoting angiogenesis and lymphangiogenesis by interacting with the chemokine receptors CXCR1 and CXCR2 to activate Akt-dependent ERK signaling [12, 13]. We investigated the effect of disulfide bonding on the ability of refp17 to promote lymphangiogenesis *in vitro*. As shown in Fig. 3, capillary-like (tube) structures formed 8 h after treatment of lymph node-derived lymphatic endothelial cells (LECs) in the presence of either refp17 or SS-p17 at 0.01 μg/ml, but none was observed at the same time in untreated cultures. Quantification of the number of tubes formed indicated that both proteins were similarly active in promoting lymphangiogenesis. Two representative B cell clonogenic NHL-

derived vp17s, characterized for amino acid insertions at position 117-118 or 125-126, namely NHL-a101 and NHL-a102, were also tested and found equally active than refp17 in promoting lymphangiogenesis. These results suggest that the pro-lymphangiogenic activity of refp17 is independent of protein structure and stability.

3.3. The functional epitope for B cell growth promoting activity is located within the refp17 N-terminus

The finding that destabilization or misfolding of refp17 or vp17s activates B cell clonogenic function led us to hypothesize that such activity may be conferred by the expression of a specific and stable epitope in vp17s which is endowed in properly folded refp17. To test this hypothesis, we chemically synthesized 8 partially overlapping peptides derived from refp17. The first 7 peptides each comprised 20 aa with 5 overlapping residues, and the C-terminal peptide contained 36 aa with 15 overlapping residues (Fig. 4A). Activity screening at a single concentration of 0.05 µg/ml identified the refp17 N-terminal peptide (Peptide F1: GARASVLSGGELDRWEKIRL) as the one endowed with B cell growth promoting activity (Fig. 4B). Further assessments on the N-terminal peptide yielded a bell-shaped dose dependency profile with maximal B cell clonogenic activity at 0.01 and 0.05 µg/ml (Fig. 4C). In a second set of experiments we sought to establish if the newly identified p17 domain responsible for B cell proliferation was interacting with the different known p17 receptors. To this aim, the eight synthetic peptides were evaluated by surface plasmon resonance (SPR) as previously described [12, 16, 17]. As shown in Fig. 4D, only one peptide out of the eight, namely Peptide F2 (sequence 17-36 aa) was able to bind simultaneously to CXCR1, CXCR2 and heparin, suggesting that this single p17 domain is crucial for the binding of the protein to all its three known receptors. It is worth noting that Peptide F2 contains the highly polybasic region of p17 – GKKQYKLKHI – already known to be involved in refp17 binding to both CXCR1 and HSPGs [16]. As expected, the B cell

clonogenic Peptide F1 was devoid of any binding activity to the known p17 receptors, thus enforcing the hypothesis of an alternate receptor(s) responsible for B cell proliferation triggered by misfolded vp17s.

3.4. B cell clonogenic activity of viral proteins is dependent on three positively charged aa

Peptide F1 is composed of a hydrophobic N-terminal region (aa 2-11) and of a hydrophilic C-terminal region (aa 12-21). In order to establish the functional residues within the Peptide F1, we synthesized different peptides in which critical aa along the entire sequence, or more specifically inside the hydrophobic or the hydrophilic regions, were substituted with Ala residues. Ala substitutions were intended to linearize and contemporarily change charges of Peptide F1 (Fig. 4E). As shown in Fig. 4F, all peptides but F1b lost their clonogenic activity, thus excluding the involvement of the hydrophobic region in the Peptide F1 clonogenic activity. Focusing our attention to the hydrophilic region, we found that the peptide clonogenic activity could be restricted to three aa residues, namely Arg, Lys and Arg at position 15, 18 and 20 respectively (Peptide F1d). To further assess the role of these residues in the Peptide F1 activity, we synthesized a peptide (F1e) in which the three aa residues were substituted with Asp instead of Ala, in order to maintain the original conformation of Peptide F1 but at the same time introducing negatively charged in place of the three positively charged aa in the peptide sequence. And indeed, when tested in the clonogenic assay, Peptide F1e did not exert any growth-promoting activity on B cells. Other F1 based peptides carrying double or single mutations instead of the three replacing the functional hydrophilic residues were synthesized and tested in the clonogenic assay. As shown in Fig. 5, whatever combination of substitutions in the three aa residues involving two of them only, did not result in the impairment of the peptide clonogenic activity. Altogether, our data support a role of the three positively charged aa residues at position 15, 18 and 20 of

the p17 N-terminal region (Fig. 5C) [37], in interacting with a hydrophobic pocket of an alternate p17 receptor.

3.5. The p17 neutralizing mAb MBS-3 impairs the Peptide F1 B cell growth-promoting activity

The clonogenic assay has its own requirements in terms of cell inoculum to ensure reliable and/or reproducible data. In our hands, the presence of antibodies or drugs in the medium gives rise to unreliable results. Therefore, in order to assess the capability of specific p17 antibodies to neutralize clonogenic activity of viral proteins and Peptide F1, we utilized a single cell cloning assay. This cloning method is performed by seeding a single B cell in each well of a 96-well plate in the presence or absence of an unrelated (Ctrl) or of the p17 neutralizing mAb MBS-3, which recognizes an epitope included in the clonogenic Peptide F1 [22]. As representatively shown in Fig. 6 (upper panels), Raji cells formed a visible single colony in > 60% of seeded wells at day 8 of culture attesting for active cell proliferation. As expected, in the presence of 0.01 μg/ml of Peptide F1, colonies showed a significantly ($P < 0.001$) larger size than colonies cultured in medium alone (NT). The presence of mAb MBS-3 (1 μg/ml) completely inhibited the clonogenic activity of Peptide F1, whereas an unrelated mAb (1 μg/ml) proved to be ineffective (Fig. 6, lower panel, left). A cell suspension was obtained by pooling equal numbers of colonies per each experimental condition and the absolute number of cells was evaluated by propidium iodide staining and flow cytometry. As shown in Fig. 6 (lower panel, right), cell proliferation significantly increased when cultured in medium containing Peptide F1 as compared to untreated (NT) cells. Peptide F1-triggered cell proliferation was inhibited by the presence of the p17 mAb MBS-3 but not by the presence of an unrelated mAb.

3.6. The B cell growth-promoting activity of the Peptide F1 is linked to activation of the Akt signaling pathway

The PI3K/Akt signaling pathway plays a crucial role in the development and malignant progression of lymphomas [38]. Because vp17s promote B cell clonogenicity and differ from refp17 for their ability to activate the Akt pathway, we explored the capability of the Peptide F1 to modulate the phosphorylation status of Akt. As shown in Fig. 7A, Raji cells stimulated for 5 min with 0.01 or 0.05 μg/ml of the Peptide F1 significantly increased the active phosphorylation of the Akt kinase compared to untreated cells (NT). At the same time, Peptide F1 at the same concentrations as above did not promote activation of the ERK1/2 kinase. To investigate further whether this pathway plays a direct role in the Peptide F1-induced B cell proliferation, we cloned Raji cells in the presence of optimal concentration of the inhibitor of Akt (Akt VIII i [1 μM]). As shown in Fig 7B, the B cell growth-promoting activity of the Peptide F1 was significantly inhibited by Akt inhibitor VIII. On the other hand, as expected, the activity of the Peptide F1 on Raji cells was not modulated by an optimal concentration of the inhibitor of mitogen-activated protein kinase (MEK)/ERK1/2 (PD98059 [10 μM]).

3.7. Replacement of Arg15, Lys18 and Arg20 with Asp removes the B cell clonogenic activity of the vp17s HNL-a101 and NHL-a102

A proof of concept experiment was run to better define the role of Arg15, Lys 18 and Arg 20 in conferring clonogenic properties to HIV-NHL-derived vp17s. Active NHL-a101 and NHL-a102 were engineered by replacing the positively charged Arg15, Lys18 and Arg20 with the negatively charged Asp and mutated vp17s were then investigated for their B cell clonogenic activity. As shown in Fig. 8, both vp17s bearing the R15D, K18D and R20D mutations, different to their natural counterparts NHL-a101 and NHL-a102, lost their capacity to enhance B cell clonogenicity.

4. Discussion

Here we demonstrate that disulfide bonding converted an inactive refp17 protein to an active one in promoting transformed B cell growth by altering and destabilizing its structure. Folding of a structural viral protein is important to sustain viral infection and replication by interacting with specific receptors and intracellular molecules and to ensure its proper incorporation into the forming virus particle. Plasticity of a structural viral protein has been always considered a mechanism to evade the immunological response but still allowing the mutated protein to continue performing its activity in sustaining virus replication into the target cell. HIV-1 escapes from specific CTL responses as the result of the expression of amino acid mutations that disrupt the normal processing [36, 39], presentation [40], or recognition [41] of the targeted CTL epitopes. At the same time, persistence of HIV-1 infection has been associated, at least in part, with change in viral envelope proteins leading to antigenic variation and escape from neutralizing antibodies [41-44]. Knowledge of the capability of structural viral proteins to exert biological properties once present as individual proteins in the extracellular microenvironment, has favoured a new way of thinking to mutated proteins as molecules that may lose specific functions or acquire new ones. This is the case of the HIV-1 matrix protein p17, which is endowed of peculiar biological activities exerted on different target cells once it is secreted in the microenvironment [8]. In a properly folded state, refp17 does not exert any biological activity on B cell growth and proliferation. However, misfolding of refp17 following the insertion of two Ala residues at position 117 [20] or a single Arg to Gly mutation at position 76 [45] results in the capability of both mutant proteins to sustain a potent B cell growth-promoting activity. Previous evidence showing that truncation of the last 36 aa residues in refp17 (Δ36) causes protein unfolding and acquisition of B cell clonogenic activity [29] let us hypothesize the presence, in refp17, of a functional but masked epitope endowed with B cell growth promoting activity. Here we confirm this

hypothesis since forcing a disulphide bridge between two Cys residues in refp17 we obtain a misfolded protein that displays a potent B cell clonogenic activity. Dissection of refp17 allowed us to identify the epitope responsible for this activity on B cells, which is located at the N-terminal region of the viral protein. Indeed, the 20 aa-long synthetic Peptide F1 mimicking the active epitope of refp17 was found to possess the capability of promoting B cell growth and proliferation. We also highlighted the critical role played by three positively charged aa, namely Arg15, Lys18 and Arg20, in sustaining the activity of Peptide F1 on B cells. Proof of concept experiments showed that these three positively charged aa residues are involved in the vp17s activity. In fact, mutation of Arg15, Lys18 and Arg20 with the negatively charged Asp led two different vp17s derived from HIV^+ NHL patients, namely NHL-a101 and NHL-a102, to completely lose their B cell clonogenic activity.

Interestingly, data on the capability of both refp17 and SS-p17 to promote angiogenesis suggests the presence of two independent functional regions in the viral protein responsible for B cell proliferation and pro-lymphangiogenic activity. This finding is supported by previous studies showing that B-cell clonogenic vp17s display angiogenic and lymphangiogenic activity through interaction with the p17 receptors CXCR1 and CXCR2 [46, 47] and by activation of autophagy [47]. Indeed, lack of any interaction of the biologically active Peptide F1 with the known refp17 receptors strongly supports the hypothesis of an alternate receptor(s) at work in sustaining vp17s activity on B cell proliferation. In particular, our data support a role of the positively charged Arg15, Lys18 and Arg20 in the interaction with a hydrophobic pocket of a still unknown receptor. This receptor(s) is likely to be not uniquely expressed on B cells, but also on other tumor cells since we recently showed that B cell clonogenic vp17s, differently from refp17, promote breast cancer cell proliferation and clonogenicity [48].

The B cell growth-promoting activity of vp17s was previously found to be concomitant to activation of the Akt signaling pathway [20]. Here we show that the Peptide F1 activates the

Akt pathway and that this pathway is responsible for its B cell growth-promoting activity. In fact, pharmacologic inhibition of the Akt signaling pathway led to a dramatic inhibition of B cell proliferation triggered by the Peptide F1. This is not surprising since previous data showed that activation of Akt pathway in B cells by clonogenic vp17s can orchestrate the function of several molecules involved in promoting lymphoma survival and proliferation [45]. Therefore, the molecular reasons for the opposite activity of vp17s and refp17 on B cell proliferation and clonogenicity may depend on the exposure or not of a functional epitope and on activation of the PI3K/Akt signaling pathway. Our findings, showing that the Akt pathway, a critical driver of lymphoma development and metastasis, is deeply involved in the clonogenic activity of some vp17s, may offer new opportunities to identify novel treatment strategies in combating HIV-related B cell lymphoma.

On our knowledge, this is the first report describing a peptide capable of activating Akt in transformed B cells. Akt is known to have predominantly antiapoptotic activity and stimulation of Akt has also been reported to prevent tissue injury in diseases with pathological apoptosis [49]. This knowledge calls for further studies aimed at investigating the role of Peptide F1 in preventing apoptosis of transformed B cells.

The p17 mAb MBS-3, which recognizes a stretch of aa incorporated in the Peptide F1 was found to completely neutralize its B cell growth-promoting activity. It is worth noting that the epitope triggering vp17s-mediated PI3K/Akt activation and proliferation in B cells falls within an hotspot of functional activity now targeted by a synthetic HIV-1 matrix protein p17-based AT20-KLH therapeutic vaccine candidate [50, 51]. Recent data have also highlighted the capability of both refp17 and vp17s to promote angiogenesis [46] and lymphangiogenesis [47], which are essential in supporting proliferation and survival of lymphoma, as well as tumor cell dissemination [52]. Antibodies against the AT20 epitope were found to neutralize the angiogenic/lymphangiogenic activity of the viral proteins [12, 13]. Altogether, these findings support the hypothesis that the synthetic minimalist therapeutic vaccine approach

against AIDS, based on the possibility to target the highly conserved AT20 epitope, may also prove useful to design a rational strategy for prevention and/or treatment of HIV-related lymphoma.

5. Conclusions

Our study opens the way to better understanding the structure-function relationship underlying the B cell clonogenic activity of some vp17s. This may favour our knowledge of the mechanisms involved in HIV-1-driven lymphomagenesis and provide the rational background for further studies aimed to assess possible mechanisms responsible for the unmasking of the B cell clonogenic epitope in vp17s. Our findings may pave the way toward the identification of the receptor(s) sustaining the activity of NHL-derived vp17s endowed with this peculiar growth-promoting property.

Funding: Associazione Italiana per la Ricerca sul Cancro (AIRC); Grant number: 20108 to Arnaldo Caruso.

Conflict of interest: The authors declare that they have no conflicts of interest with the contents of this article.

References

1. Bonnet, F., Burty, C., Lewden, C., Costagliola, D., May, T., Bouteloup, V., Rosenthal, E., Jougla, E., Cacoub, P., Salmon, D., Chêne, G., Morlat, P., Agence Nationale de Recherches sur le Sida et les Hépatites Virales EN19 Mortalité Study Group. Mortavic Study Group. Changes in cancer mortality among HIV-infected patients: the Mortalité 2005 Survey. Clin. Infect. Dis. 48 (2009) 633-639.
2. Shiels, M.S., Pfeiffer, R.M., Gail, M.H., Hall, H.I., Li, J., Chaturvedi, A.K., Bhatia, K., Uldrick, T.S., Yarchoan, R., Goedert, J.J., Engels, EA. Cancer burden in the HIV-infected population in the United States. J. Natl. Cancer. Inst. 103 (2011) 753-762.
3. Simard, E.P., Pfeiffer, R.M., Engels, E.A. Cumulative incidence of cancer among individuals with acquired immunodeficiency syndrome in the United States. Cancer. 117 (2011) 1089-1096.
4. Cesarman, E. Gammaherpesvirus and lymphoproliferative disorders in immunocompromised patients. Cancer Lett. 305 (2011) 163-174.
5. Gloghini, A., Dolcetti, R., Carbone, A. Lymphomas occurring specifically in HIV-infected patients: from pathogenesis to pathology. Semin. Cancer. Biol. 23 (2013) 457-467.
6. Epeldegui, M., Vendrame, E., Martínez-Maza, O. HIV-associated immune dysfunction and viral infection: role in the pathogenesis of AIDS-related lymphoma. Immunol. Res. 48 (2010) 72-83.
7. Fiorentini, S., Marini, E., Caracciolo, S., Caruso, A. Functions of the HIV-1 matrix protein p17. New. Microbiol. 29 (2006) 1-10.
8. Caccuri, F., Iaria, M.L., Campilongo, F., Varney, K., Rossi, A., Mitola, S., Schiarea, S., Bugatti, A., Mazzuca, P., Giagulli, C., Fiorentini, S., Lu, W., Salmona, M., Caruso A. Cellular aspartyl proteases promote the unconventional secretion of biologically active HIV-1 matrix protein p17. Sci. Rep. 6 (2016) 38027.

9. Fiorentini, S., Riboldi, E., Facchetti, F., Avolio, M., Fabbri, M., Tosti, G., Becker, P.D., Guzman, C.A., Sozzani, S., Caruso, A. HIV-1 matrix protein p17 induces human plasmacytoid dendritic cells to acquire a migratory immature cell phenotype. Proc. Natl. Acad. Sci. U.S. A. 105 (2008) 3867-72.
10. Popovic, M., Tenner-Racz, K., Pelser, C., Stellbrink, H.J., van Lunzen, J., Lewis, G., Kalyanaraman, V.S., Gallo, R.C., Racz, P. Persistence of HIV-1 structural proteins and glycoproteins in lymph nodes of patients under highly active antiretroviral therapy. Proc. Natl. Acad. Sci. U.S.A. 102 (2005) 14807-14812.
11. Carroll, V.A., Lafferty, M.K., Marchionni, L., Bryant, J.L., Gallo, R.C., Garzino-Demo, A. Expression of HIV-1 matrix protein p17 and association with B-cell lymphoma in HIV-1 transgenic mice. Proc. Natl. Acad. Sci. U.S.A. 113 (2016) 13168-13173.
12. Caccuri, F., Giagulli, C., Bugatti, A., Benetti, A., Alessandri, G., Ribatti, D., Marsico, S., Apostoli, P., Slevin, M.A., Rusnati, M., Guzman, C.A., Fiorentini, S., Caruso, A. HIV-1 matrix protein p17 promotes angiogenesis via chemokine receptors CXCR1 and CXCR2. Proc. Natl. Acad. Sci. U.S.A. 109 (2012) 14580-14585.
13. Caccuri, F., Rueckert, C., Giagulli, C., Schulze, K., Basta, D., Zicari, S., Marsico, S., Cervi, E., Fiorentini, S., Slevin, M., Guzman, C.A., Caruso, A. HIV-1 matrix protein p17 promotes lymphangiogenesis and activates the endothelin-1/endothelin B receptor axis. Arterioscler. Thromb. Vasc. Biol. 34 (2014) 846-856.
14. Basta, D., Latinovic, O., Lafferty, M.K., Sun, L., Bryant, J., Lu, W., Caccuri, F., Caruso, A., Gallo, R., Garzino-Demo, A. Angiogenic, lymphangiogenic and adipogenic effects of HIV-1 matrix protein p17. Pathog. Dis. 73 (2015) ftv062.
15. Fiorentini, S., Giagulli, C., Caccuri, F., Magiera, A.K., Caruso, A. HIV-1 matrix protein p17: a candidate antigen for therapeutic vaccines against AIDS. Pharmacol. Ther. 128 (2010) 433-444.

16. Bugatti, A., Giagulli, C., Urbinati, C., Caccuri, F., Chiodelli, P., Oreste, P., Fiorentini, S., Orro, A., Milanesi, L., D'Ursi, P., Caruso, A., Rusnati, M. Molecular interaction studies of HIV-1 matrix protein p17 and heparin: identification of the heparin-binding motif of p17 as a target for the development of multitarget antagonists. J. Biol. Chem. 288 (2013) 1150-1161.

17. Giagulli, C., Magiera, A.K., Bugatti, A., Caccuri, F., Marsico, S., Rusnati, M., Vermi, W., Fiorentini, S., Caruso, A. HIV-1 matrix protein p17 binds to the IL-8 receptor CXCR1 and shows IL-8-like chemokine activity on monocytes through Rho/ROCK activation. *Blood*. 119 (2012) 2274-2283.

18. Totonchy, J., Cesarman, E. Does persistent HIV replication explain continued lymphoma incidence in the era of effective antiretroviral therapy?. Curr. Opin. Virol. 20, (2016) 71-77.

19. Giombini, E., Dolcetti, R., Caccuri, F., Selleri, M., Rozera, G., Abbate, I., Bartolini, B., Martorelli, D., Faè, D.A., Fiorentini, S., Giagulli, C., Capobianchi, M.R., Caruso, A. Detection of HIV-1 matrix protein p17 quasispecies variants in plasma of chronic HIV-1-infected patients by ultra-deep pyrosequencing. J. Acquir. Immune. Defic. Syndr. 66, (2014) 332-339.

20. Dolcetti, R., Giagulli, C., He, W., Selleri, M., Caccuri, F., Eyzaguirre, L.M., Mazzuca, P., Corbellini, S., Campilongo, F., Marsico, S., Giombini, E., Muraro, E., Rozera, G., De Paoli, P., Carbone, A., Capobianchi, M.R., Ippolito, G., Fiorentini, S., Blattner, W.A., Lu, W., Gallo, R.C., Caruso, A. Role of HIV-1 matrix protein p17 variants in lymphoma pathogenesis. Proc. Natl. Acad. Sci. U.S.A. 112, (2015) 14331-14336.

21. Lu, W.Y., Starovasnik, M.A., Dwyer, J.J., Kossiakoff, A.A., Kent, S.B., Lu, W. Deciphering the role of the electrostatic interactions involving Gly70 in eglin C by total chemical protein synthesis. Biochemistry. 39 (2000) 3575-3584.

22. De Francesco, M.A., Baronio, M., Fiorentini, S., Signorini, C., Bonfanti, C., Poiesi, C., Popovic, M., Grassi, M., Garrafa, E., Bozzo, L., Lewis, G.K., Licenziati, S., Gallo, R.C., Caruso, A. HIV-1 matrix protein p17 increases the production of proinflammatory cytokines and counteracts IL-4 activity by binding to a cellular receptor. Proc. Natl. Acad. Sci. U.S.A. 99, (2002) 9972-9977.

23. Wu, Z., Alexandratos, J., Ericksen, B., Lubkowski, J., Gallo, R.C., Lu, W. Total chemical synthesis of N-myristoylated HIV-1 matrix protein p17: structural and mechanistic implications of p17 myristoylation. Proc. Natl. Acad. Sci. U.S.A. 101, (2004) 11587-11592.

24. Caruso, A., Caselli, E., Fiorentini, S., Rotola, A., Prandini, A., Garrafa, E., Saba, E., Alessandri, G., Cassai, E., Di Luca, D. U94 of human herpesvirus 6 inhibits in vitro angiogenesis and lymphangiogenesis. Proc. Natl. Acad. Sci. U.S.A. 106, (2009) 20446-20451.

25. Marion, D., Driscoll, P.C., Kay, L.E., Wingfield, P.T., Bax, A., Gronenborn, A.M., Clore, G.M. Overcoming the overlap problem in the assignment of 1H NMR spectra of larger proteins by use of three-dimensional heteronuclear 1H-15N Hartmann-Hahn-multiple quantum coherence and nuclear Overhauser-multiple quantum coherence spectroscopy: application to interleukin 1 beta. Biochemistry. 28 (1989) 6150-6156.

26. Bax, A., Ikura, M. An efficient 3D NMR technique for correlating the proton and 15N backbone amide resonances with the alpha-carbon of the preceding residue in uniformly 15N/13C enriched proteins. J. Biomol. NMR. 1 (1991) 99-104.

27. Delaglio, F., Grzesiek, S., Vuister, G.W., Zhu, G., Pfeifer, J., Bax, A. NMRPipe: a multidimensional spectral processing system based on UNIX pipes. J. Biomol. NMR. 6 (1995) 277-293.

28. Mori, S., Abeygunawardana, C., Johnson, M.O., van Zijl, P.C. Improved sensitivity of HSQC spectra of exchanging protons at short interscan delays using a new fast HSQC

(FHSQC) detection scheme that avoids water saturation. J. Magn. Reson. *B.* 108 (1995) 94-98.

29. Giagulli, C., Marsico, S., Magiera, A.K., Bruno, R., Caccuri, F., Barone, I., Fiorentini, S., Andò, S., Caruso, A. Opposite effects of HIV-1 p17 variants on PTEN activation and cell growth in B cells. PLoS One. 14, (2011) e17831.
30. Saad, J.S., Ablan, S.D., Ghanam, R.H., Kim, A., Andrews, K., Nagashima, K., Soheilian, F., Freed, E.O., Summers, M.F. Structure of the myristylated human immunodeficiency virus type 2 matrix protein and the role of phosphatidylinositol-(4,5)-bisphosphate in membrane targeting. J. Mol. Biol. 382, (2008) 434-447.
31. LaPlante, S.R., Forgione, P., Boucher, C., Coulombe, R., Gillard, J., Hucke, O., Jakalian, A., Joly, M.A., Kukolj, G., Lemke, C., McCollum, R., Titolo, S., Beaulieu, P.L., Stammers, T. Enantiomeric atropisomers inhibit HCV polymerase and/or HIV matrix: characterizing hindered bond rotations and target selectivity. J. Med. Chem. 57 (2014) 1944-1951.
32. Hill, C.P., Worthylake, D., Bancroft, D.P., Christensen, A.M., Sundquist, W.I. Crystal structures of the trimeric human immunodeficiency virus type 1 matrix protein: implications for membrane association and assembly. Proc. Natl. Acad. Sci. U.S.A. 93 (1996) 3099-3104.
33. Tam, P.J., Wu, C., Liu, W., Zhang, J. Disulfide Bond Formation in Peptides by Ddimethyl Sulfoxide. Scope and Application. J. Am. Chem. Soc. 113 (1991) 6657-6662.
34. Wu, Z., Powell, R., Lu, W. Productive folding of human neutrophil alpha-defensins in vitro without the pro-peptide. J. Am. Chem. Soc. 125 (2003) 2402-2403.
35. Wu, Z., Hoover, D.M., Yang, D., Boulegue, C., Santamaria, F., Oppenheim, J.J., Lubkowski, J., Lu, W. Engineering disulfide bridges to dissect antimicrobial and

chemotactic activities of human β-defensin 3. Proc. Natl. Acad. Sci. U.S.A. 100 (2003) 8880-8885.

36. Massiah, M.A., Starich, M.R., Paschall, C., Summers, M.F., Christensen, A.M., Sundquist, W.I. Three-dimensional structure of the human immunodeficiency virus type 1 matrix protein. J. Mol. Biol. 244 (1994) 198-223.
37. Matthews, S., Barlow, P., Clark, N., Kingsman, S., Kingsman, A., Campbell, I. Refined solution structure of p17, the HIV matrix protein. Biochem. Soc. Trans. 23 (1995) 725-729.
38. Jiang, B.H., Liu, L.Z. PI3K/PTEN signaling in tumorigenesis and angiogenesis. Biochim. Biophys. Acta. 1784 (2008) 150-158.
39. Allen, T.M., Altfeld, M., Yu, X.G., O'Sullivan, K.M., Lichterfeld, M., Le Gall, S., John, M., Mothe, B.R., Lee, P.K., Kalife, E.T., Cohen, D.E., Freedberg, K.A., Strick, D.A., Johnston, M.N., Sette, A., Rosenberg, E.S., Mallal, S.A., Goulder, P.J., Brander, C., Walker, B.D. Selection, transmission, and reversion of an antigen-processing cytotoxic T-lymphocyte escape mutation in human immunodeficiency virus type 1 infection. J. Virol. 78 (2004) 7069-7078.
40. Leslie, A., Kavanagh, D., Honeyborne, I., Pfafferott, K., Edwards, C., Pillay, T., Hilton, L., Thobakgale, C., Ramduth, D., Draenert, R., Le Gall, S., Luzzi, G., Edwards, A., Brander, C., Sewell, A.K., Moore, S., Mullins, J., Moore, C., Mallal, S., Bhardwaj, N., Yusim, K., Phillips, R., Klenerman, P., Korber, B., Kiepiela, P., Walker, B., Goulder, P. Transmission and accumulation of CTL escape variants drive negative associations between HIV polymorphisms and HLA. J. Exp. Med. 201 (2005) 891-902.
41. Yang, O.O., Sarkis, P.T., Ali, A., Harlow, J.D., Brander, C., Kalams, S.A., Walker, B.D. Determinant of HIV-1 mutational escape from cytotoxic T lymphocytes. J. Exp. Med. 197 (2003) 1365-1375.

42. Cohen, J. HIV. Escape artist par excellence. Science. 299 (2003) 1505-1508.

43. Kalia, V., Sarkar, S., Gupta, P., Montelaro, R.C. Antibody neutralization escape mediated by point mutations in the intracytoplasmic tail of human immunodeficiency virus type 1 gp41. J. Virol. 79 (2005) 2097-2107.

44. Wibmer, C.K., Bhiman, J.N., Gray, E.S., Tumba, N., Abdool Karim, S.S., Williamson, C., Morris, L., Moore, P.L. Viral escape from HIV-1 neutralizing antibodies drives increased plasma neutralization breadth through sequential recognition of multiple epitopes and immunotypes. PLoS Pathog. 9 (2013) e1003738.

45. Giagulli C, D'Ursi P, He W, Zorzan S, Caccuri F, Varney K, Orro A, Marsico S, Otjacques B, Laudanna C, Milanesi L, Dolcetti R, Fiorentini S, Lu W, Caruso A. A single amino acid substitution confers B-cell clonogenic activity to the HIV-1 matrix protein p17. Sci. Rep. 7 (2017) 6555.

46. Caccuri, F., Giagulli, C., Reichelt, J., Martorelli, D., Marsico, S., Bugatti, A., Barone, I., Rusnati, M., Guzman, C.A., Dolcetti, R., Caruso, A. Simian immunodeficiency virus and human immunodeficiency virus type 1 matrix proteins specify different capabilities to modulate B cell growth. J. Virol. 88 (2014) 5706-5717.

47. Mazzuca, P., Marsico, S., Schulze, K., Mitola, S., Pils, M.C., Giagulli, C., Guzman, C.A., Caruso, A., Caccuri, F. Role of Autophagy in HIV-1 Matrix Protein p17-Driven Lymphangiogenesis. J. Virol. 91 (2017) pii:e00801-17.

48. Caccuri, F., Giordano, F., Barone, I., Mazzuca, P., Giagulli, C., Andò, S., Caruso, A., Marsico, S. HIV-1 matrix protein p17 and its variants promote human triple negative breast cancer cell aggressiveness. Infect. Agent. Cancer. 12 (2017) 49.

49. McDunn, J.E., Muenzer, J.T., Rachdi, L., Chang, K.C., Davis, C.G., Dunne, W.M., Piwnica-Worms, D., Bernal-Mizrachi, E., Hotchkiss, R.S. Peptide-mediated activation of Akt and extracellular regulated kinase signaling prevents lymphocyte apoptosis. FASEB J. 22 (2008) 561.

50. Fiorentini, S., Marini, E., Bozzo, L., Trainini, L., Saadoune, L., Avolio, M., Pontillo, A., Bonfanti, C., Sarmientos, P., Caruso, A. Preclinical studies on immunogenicity of the HIV-1 p17-based synthetic peptide AT20-KLH. Biopolymers. 76 3(2004) 34-343.
51. Iaria, M.L., Fiorentini, S., Focà, E., Zicari, S., Giagulli, C., Caccuri, F., Francisci, D., Di Perri, G., Castelli, F., Baldelli, F., Caruso, A. Synthetic HIV-1 matrix protein p17-based AT20-KLH therapeutic immunization in HIV-1-infected patients receiving antiretroviral treatment: A phase I safety and immunogenicity study. Vaccine. 32, (2014) 1072-1078.
52. Pepper, M.S., Tille, J.C., Nisato, R., Skobe, M. Lymphangiogenesis and tumor metastasis. Cell. Tissue. Res. 314 (2003) 166-177.

Figure legends

Figure 1. Comparison of recombinant and synthetic refp17 structure and activity. (A) Crystal structure of refp17 with Cys57 and Cys87 shown as balls. (B) Blow-up of Cys57 and Cys87 in refp17 showing a distance of 9.7 Å between the two sulfur atoms. (C) Two-dimensional NMR spectroscopic analysis of recombinant refp17 (black) and synthetic refp17 (red). Signals of Hα-HN (aliphatic-amide) nuclear Overhauser effects (NOEs) are shown on the left, and HN-HN (amide-amide) NOEs on the right. Nearly all HN-HN cross signals of synthetic refp17 (red, right) are superimposable with those of recombinant refp17 (black, right), suggesting that the structures of the two proteins are highly similar, if not identical. (D) Raji cells were plated in 12-well plates, and after 4 d, medium was replaced by fresh medium with various concentrations, 0.01, 0.05, and 0.1 μg/ml, of recombinant and synthetic refp17. Cells not treated (NT) were used as negative control. The cell growth was analyzed by using MTT. Data represent the average number of colonies ± SD from three independent experiments performed in triplicate. The statistical significance between control and treated cultures was calculated using one-way ANOVA performed separately for each concentration of protein across the three groups. Bonferroni's post-test was used to compare data. *$P < 0.05$, **$P < 0.01$.

Figure 2. Biophysical and biological characterization of refp17 and SS-p17. (A) Circular dichroism spectra of refp17 and SS-p17 obtained at 25 °C. Alpha-helicity is characterized by two negative peaks at 208 and 222 nm and one positive peak at 195 nm. (B) GuHCl-induced chemical denaturation of refp17 and SS-p17 monitored at room temperature by CD spectroscopy at 222 nm. (C) Heat-induced thermal denaturation of refp17 and SS-p17 monitored by CD spectroscopy at 222 nm. (D) The aliphatic-aliphatic NOESY NMR spectra of refp17 (black) and SS-p17 (red) collected at 25 °C. (E) The amide-amide NOESY NMR spectra of refp17 (black) and SS-p17 (red) collected at 25 °C. (F) Molecular sizes of refp17 and SS-17 in solution measured by dynamic light scattering

techniques. (G) Raji (left panel) and BJAB (right panel) cells were plated in 12-well plates, and after 4 d, medium was replaced by fresh medium with various concentrations, 0.01, 0.05, and 0.1 µg/ml, of recombinant refp17 or SS-p17. Cells not treated (NT) were used as negative control. The cell growth was analyzed by using 3-[4, 5-Dimethylthiazol-2-y1]-2, 5-diphenyltetrazolium bromide (MTT). Data represent the average number of colonies ± SD from three independent experiments performed in triplicate. The statistical significance between control and treated cultures was calculated using one-way ANOVA performed separately for each concentration of proteins across the three groups. Bonferroni's post-test was used to compare data. *P < 0.05, **P < 0.01, ***P < 0.001.

Figure 3. All vp17s display the same ability of refp17 to induce capillary-like structures formation. Lymph nodes lymphatic endothelial cells (LN-LECs) were starved for 24 h and then stimulated or not with refp17, SS-p17, NHL-a101 or NHL-a102 (0.01 µg/ml) in complete medium. Pictures were taken after 8 h of culture on growth factor-reduced Cultrex BME (original magnification, x10) and are representative of three independent experiments with similar results. Values reported for LN-LEC capillary-like structure (tube) formation are the means ± SD of three independent experiments with similar results. Statistical analysis was performed by one-way ANOVA, and the Bonferroni post-test was used to compare data. ***P < 0.001. NT indicates not treated cells.

Figure 4. Ability of different p17-derived peptides to induce B cell clonogenicity and to bind to refp17 receptors. (A) Schematic representation of 8 p17-derived peptides. Raji cells were plated in 12-well plates, and after 4 days, medium was replaced by fresh medium containing (B) 0.05 µg/ml of each p17-derived peptides (F1, F2, F3, F4, F5, F6, F7, F8) or (C) various concentration of Peptide F1 (0.001, 0.01, 0.05, 0.1, 0.5 µg/ml). Cells not treated (NT) were used as negative control. Cell proliferation was analyzed by using MTT. Data represent the average number of colonies ± SD from three independent experiments performed in triplicate. The statistical significance between

control and treated cultures was calculated using one-way ANOVA performed separately for each concentration of p17-derived peptides across the three groups. Bonferroni's post-test was used to compare data. *P < 0.05, **P < 0.01. (D) SPR analysis of the interaction of p17-derived peptides with p17 receptors. SPR sensorgrams of 1 to 8 peptides on CXCR1 (upper panel), CXCR2 (middle panel) and heparin (lower panel). In the figure was reported the injection start point (black arrows) and the point of the end of injection (withe arrows) for all peptides. (E) Amino acid substitutions in the Peptide F1 analyzed in this study. The reference sequence is shown by using single-letter amino acid code. The name of the mutant and the changes in the amino acid sequence are shown. Dots represent unchanged sequence. (F) Raji cells were plated in 12-well plates, and after 4 days, medium was replaced by fresh medium with 0.05 μg/ml of Peptide F1, F1a, F1b, F1c, F1d or F1e. Cells not treated (NT) were used as negative control. The cell growth was analyzed by using MTT. Data represent the average number of colonies ± SD from three independent experiments performed in triplicate. The statistical significance between control and treated cultures was calculated using one-way ANOVA and the Bonferroni's post-test was used to compare data. **P < 0.01, ***P < 0.001.

Figure 5. The combination of three critical amino acids mutations in the Peptide F1 are required for its clonogenic activity. (A) Amino acid substitutions in the Peptide F1 analyzed in this study. The reference sequence is shown by using single-letter amino acid code. The name of the mutant and the changes in the amino acid sequence are shown. Dots represent unchanged sequence. (B) Raji cells were plated in 12-well plates, and after 4 days, medium was replaced by fresh medium with various concentrations of different peptides. Cells not treated (NT) were used as negative control. The cell growth was analyzed by using MTT. Data represent the average number of colonies ± SD from three independent experiments performed in triplicate. The statistical significance between control and treated cultures was calculated using one-way ANOVA performed separately for each concentration of proteins across the three groups. Bonferroni's post-test was used to compare data.

*P < 0.05, **P < 0.01, ***P < 0.001. (C) NMR structure of refp17 with Arg15, Lys18, Arg20, Cys57 and Cys87 shown in balls, prepared using PyMol from the PDB code 1TAM.

Figure 6. Specificity of Peptide F1 activity on B cells. Raji cells form colonies when sorted into 96 well plates as single cell. Plates were cultured for 8 d in the presence or absence of Peptide F1 (0.01µg/ml). For some experimental condition the Peptide F1 was pre-incubated for 30 min at 37 °C with 1 µg/ml of unrelated control mAb (Ctrl mAb) or p17 neutralizing mAb MBS-3. Bright-field images represent the characteristic morphology of 2D colonies (upper panels), one colony for each condition is shown (original magnification, x40). The colony area was measured (15 colonies/condition) by using Leica Qwin image analysis software (lower panel, left graph). The same number of colonies (15 colonies/condition) was aseptically harvested from 96-well plates and stained with Propidium Iodide (PI) to detect PI^- viable cells by flow cytometry (lower panel, right graph). Absolute cell counts were obtained by the counting function of the MACSQuant® Analyzer. Cells not treated (NT) were used as negative control. Data are representative of three independent experiments performed in triplicate. The statistical significance between control and treated cultures was calculated using one-way ANOVA and the Bonferroni's post-test was used to compare data. ***P < 0.001.

Figure 7. The Peptide F1 promotes B cell proliferation through activation of the Akt signaling pathway. (A) Raji cells were treated for 1 and 5 min with 0.01 or 0.05 µg/ml of the Peptide F1 and then lysed. Untreated cells were used as control. Equal amounts of total cellular extracts were analyzed for expression of pAkt, Akt, pERK1/2 or ERK1/2 by western blot analysis using mAbs to pAkt (Ser473), Akt, pERK1/2 (Thr202/Tyr204) or ERK1/2 as specific reagents. Phosphorylation of Akt, and ERK1/2 was verified by densiometric analysis and plotting of the pAkt/Akt, and pERK1/2/ERK1/2. Blots from one representative experiment of three with similar results are shown (left panels). Values reported for pAkt and pERK1/2 are the mean ± SD of three independent

experiments with similar results (right panels). Statistical analysis was performed by one-way ANOVA, and the Bonferroni post-test was used to compare data. *P < 0.05, **P < 0.01. (B) Raji cells were cultured for 8 days in the presence or absence of the Peptide F1 (0.01μg/ml) alone or in combination with inhibitor of Akt (Akt VIII i) (1 μM) or inhibitor of MEK/ERK1/2 (PD98059) (10 μM) signaling pathways. Bright-field images represent the characteristic morphology of 2D colonies (upper panels), one colony for each condition is shown (original magnification, x40). The colony area was measured (15 colonies/condition) by using Leica Qwin image analysis software (lower panel, left). The same number of colonies (15 colonies/condition) was aseptically harvested from 96-well plates and stained with Propidium Iodide (PI) to detect PI^- viable cells by flow cytometry (lower panel, right). Absolute cell counts were obtained by the counting function of the MACSQuant® Analyzer. Cells not treated (NT) were used as negative control. Data are representative of three independent experiments performed in triplicate. The statistical significance between control and treated cultures was calculated using one-way ANOVA and the Bonferroni's post-test was used to compare data. ***P < 0.001.

Figure 8. Critical amino acids mutations in the clonogenic epitope of vp17s induce a not-clonogenic activity. Raji cells were plated in 12-well plates, and after 4 d, medium was replaced by fresh medium with various concentrations, 0.01, 0.05, and 0.1 μg/ml, of recombinant refp17, NHL-a101, NHL-a101mutDDD, NHL-a102, or NHL-a102mutDDD. Cells not treated (NT) were used as negative control. The cell growth was analyzed by using MTT. Data represent the average number of colonies ± SD from three independent experiments performed in triplicate. The statistical significance between control and treated cultures was calculated using one-way ANOVA performed separately for each concentration of proteins across the three groups. Bonferroni's post-test was used to compare data. **P < 0.01, ***P < 0.001.

Highlights:

- The HIV-1 p17 has a masked epitope endowed with B cell growth promoting activity
- Three amino acids are indispensable for the B cell proliferative activity of p17
- P17 activity on B cell proliferation depends on Akt activation

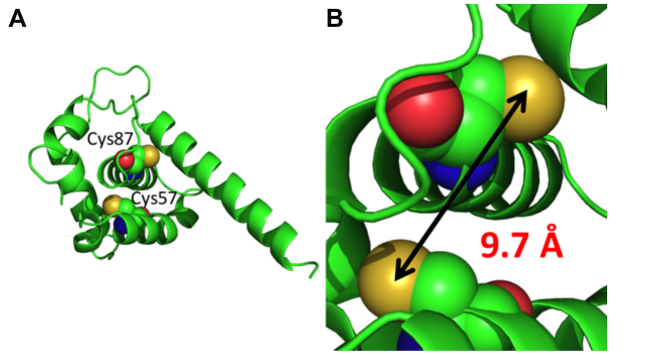
A
Cys87
Cys57
B
9.7 Å

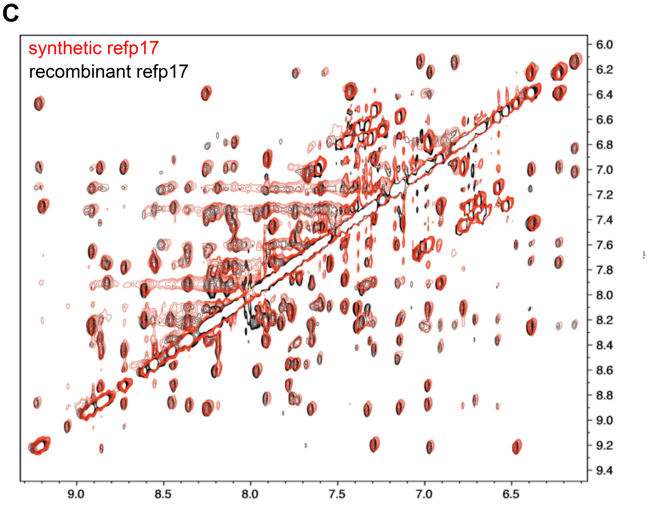
C
synthetic refp17
recombinant refp17
6.0
6.2
6.4
6.6
6.8
7.0
7.2
7.4
7.6
7.8
8.0
8.2
8.4
8.6
8.8
9.0
9.2
9.4
9.0
8.5
8.0
7.5
7.0
6.5

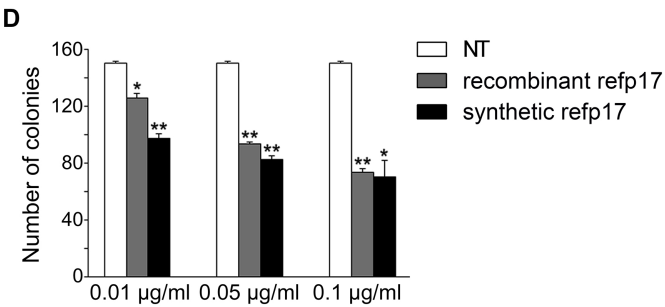
D
Number of colonies
160
120
80
40
0
0.01 µg/ml
0.05 µg/ml
0.1 µg/ml
NT
recombinant refp17
synthetic refp17
*
**

Figure 1

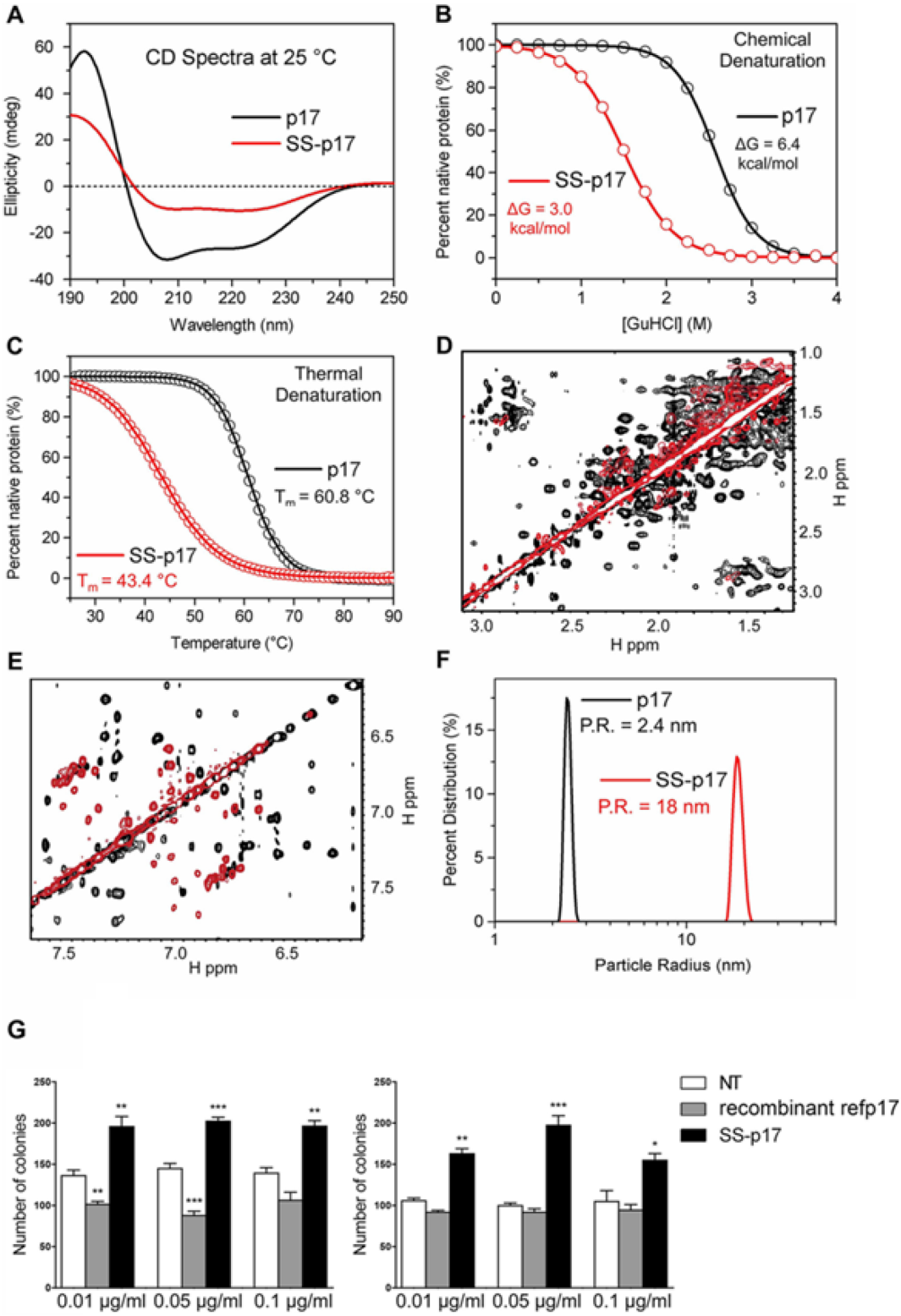
A
CD Spectra at 25 °C
p17
SS-p17
Ellipticity (mdeg)
Wavelength (nm)
B
Chemical Denaturation
p17
ΔG = 6.4 kcal/mol
SS-p17
ΔG = 3.0 kcal/mol
Percent native protein (%)
[GuHCl] (M)
C
Thermal Denaturation
p17
Tm = 60.8 °C
SS-p17
Tm = 43.4 °C
Percent native protein (%)
Temperature (°C)
D
H ppm
H ppm
E
H ppm
H ppm
F
p17
P.R. = 2.4 nm
SS-p17
P.R. = 18 nm
Percent Distribution (%)
Particle Radius (nm)
G
NT
recombinant refp17
SS-p17
Number of colonies
0.01 µg/ml
0.05 µg/ml
0.1 µg/ml
Number of colonies
0.01 µg/ml
0.05 µg/ml
0.1 µg/ml

Figure 2

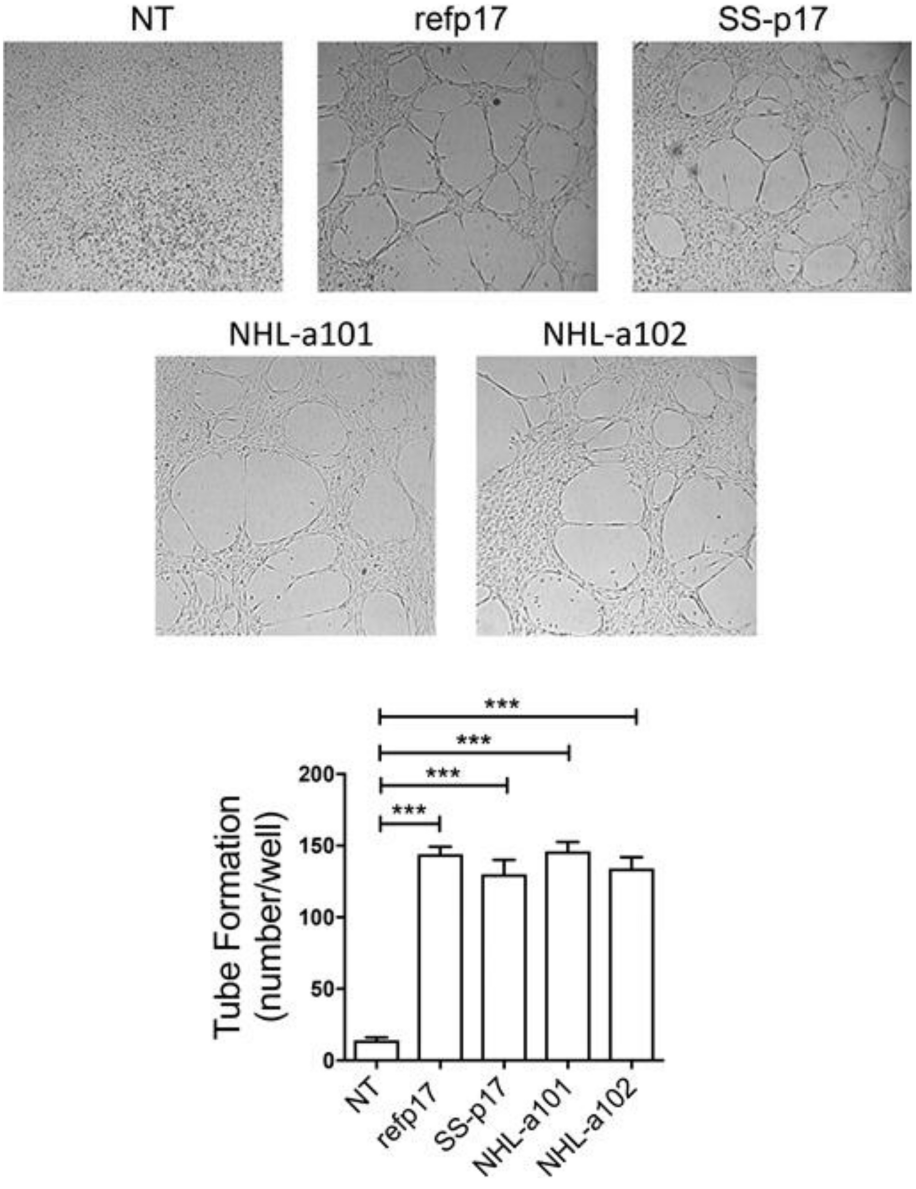
NT
refp17
SS-p17
NHL-a101
NHL-a102
***
***
***
***
Tube Formation
(number/well)
200
150
100
50
0
NT
refp17
SS-p17
NHL-a101
NHL-a102

Figure 3

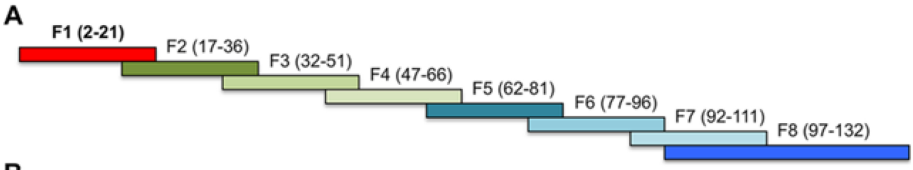
A
F1 (2-21)
F2 (17-36)
F3 (32-51)
F4 (47-66)
F5 (62-81)
F6 (77-96)
F7 (92-111)
F8 (97-132)

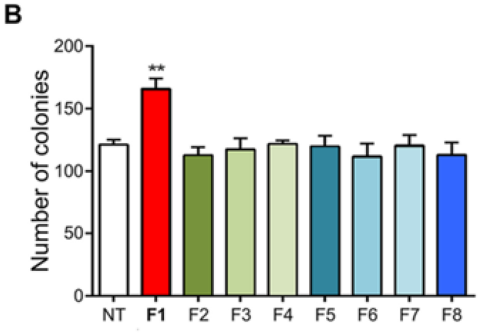
B
Number of colonies
200
150
100
50
0
**
NT
F1
F2
F3
F4
F5
F6
F7
F8

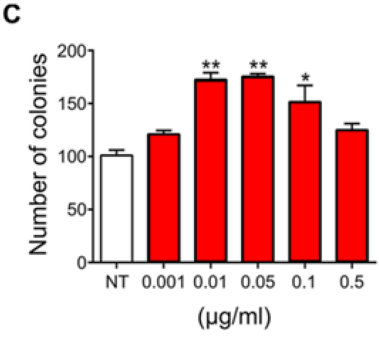
C
Number of colonies
200
150
100
50
0
**
**
*
NT
0.001
0.01
0.05
0.1
0.5
(µg/ml)

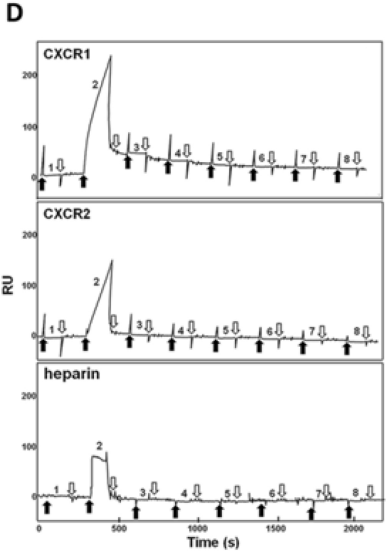
D
CXCR1
CXCR2
heparin
RU
Time (s)
0
500
1000
1500
2000

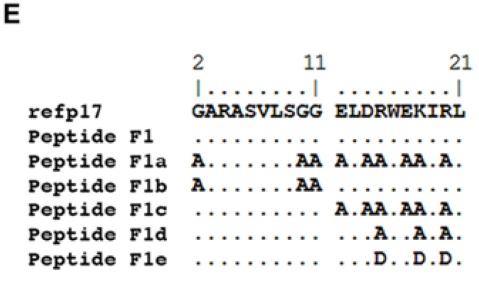
E
2
11
21
refp17 GARASVLSGG ELDRWEKIRL
Peptide F1 ....
Peptide F1a A.......AA A.AA.AA.A.
Peptide F1b A.......AA ....
Peptide F1c .... A.AA.AA.A.
Peptide F1d ....A..A.A.
Peptide F1e ....D..D.D.

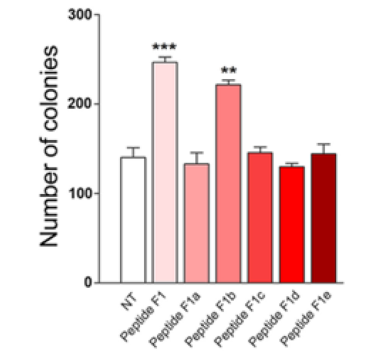
F
Number of colonies
300
200
100
0
***
**
NT
Peptide F1
Peptide F1a
Peptide F1b
Peptide F1c
Peptide F1d
Peptide F1e

Figure 4

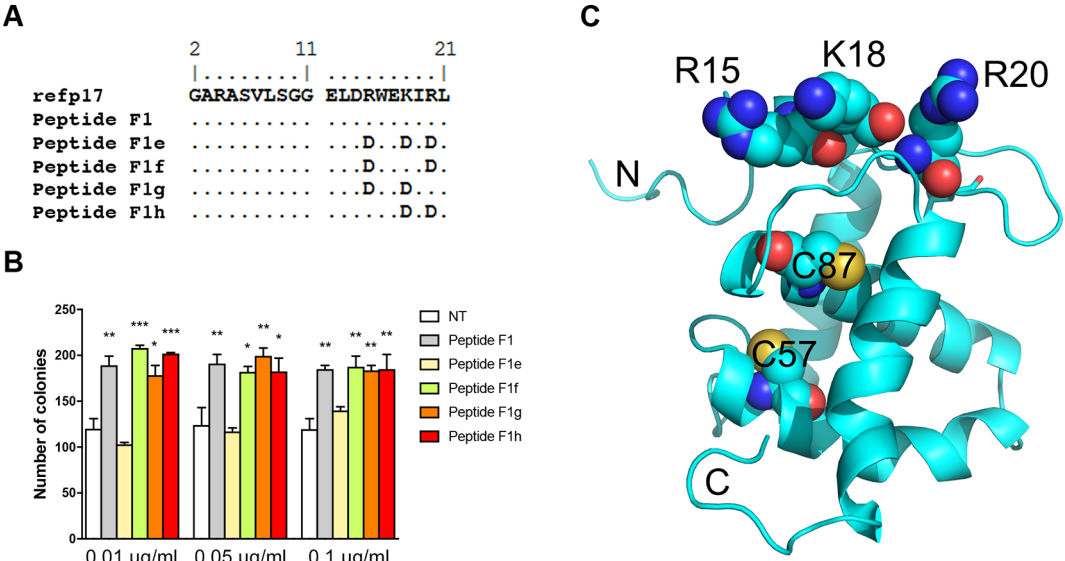
A
2 11 21
refp17 GARASVLSGG ELDRWEKIRL
Peptide F1 .....
Peptide F1e ...D..D.D.
Peptide F1f ...D....D.
Peptide F1g ...D..D...
Peptide F1h .....D.D.
B
Number of colonies
0
50
100
150
200
250
0.01 µg/ml
0.05 µg/ml
0.1 µg/ml
NT
Peptide F1
Peptide F1e
Peptide F1f
Peptide F1g
Peptide F1h
C
R15
K18
R20
N
C87
C57
C

Figure 5

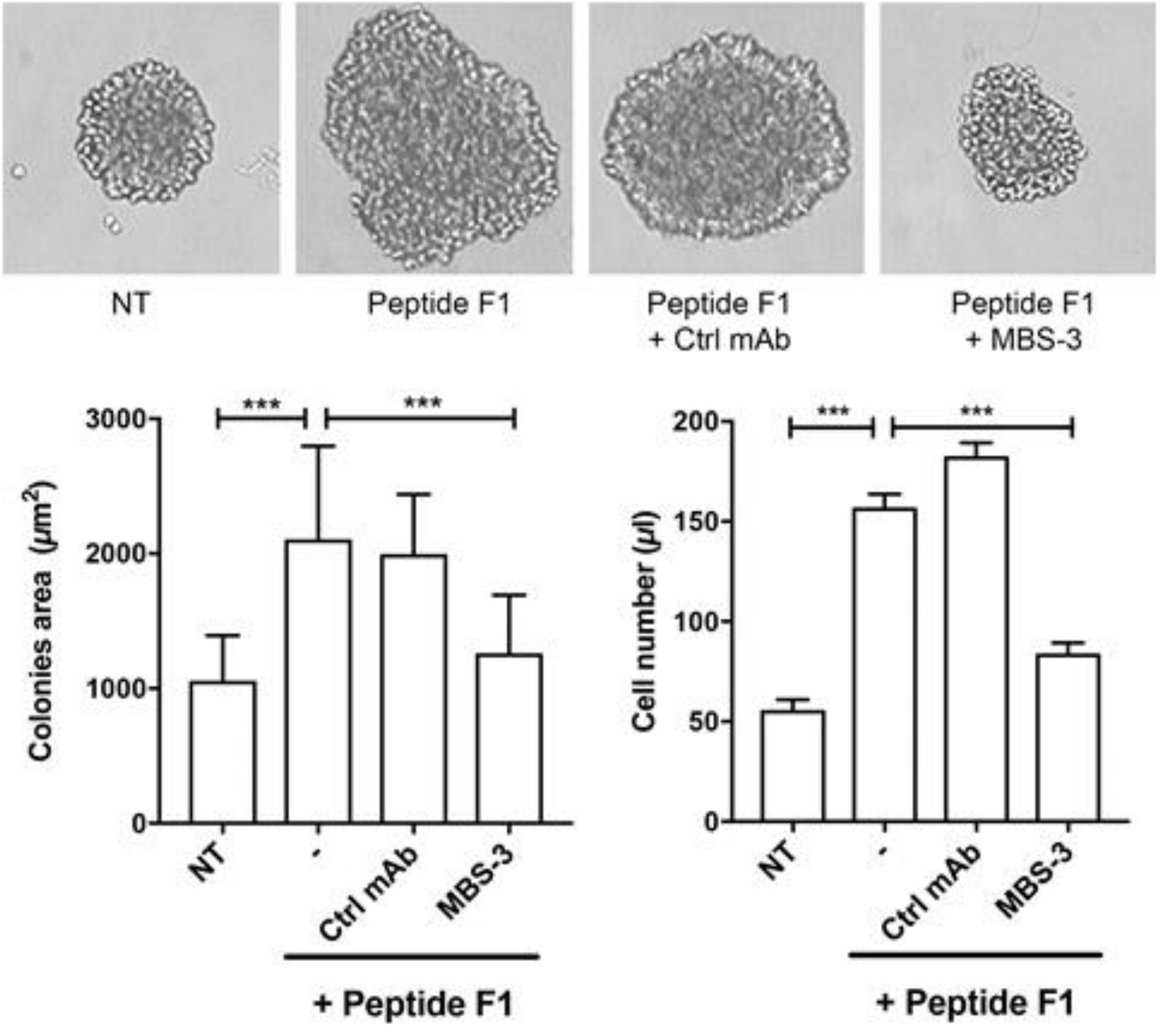
NT
Peptide F1
Peptide F1
+ Ctrl mAb
Peptide F1
+ MBS-3
Colonies area (μm²)
3000
2000
1000
0
***
***
NT
-
Ctrl mAb
MBS-3
+ Peptide F1
Cell number (μl)
200
150
100
50
0
***
***
NT
-
Ctrl mAb
MBS-3
+ Peptide F1

Figure 6

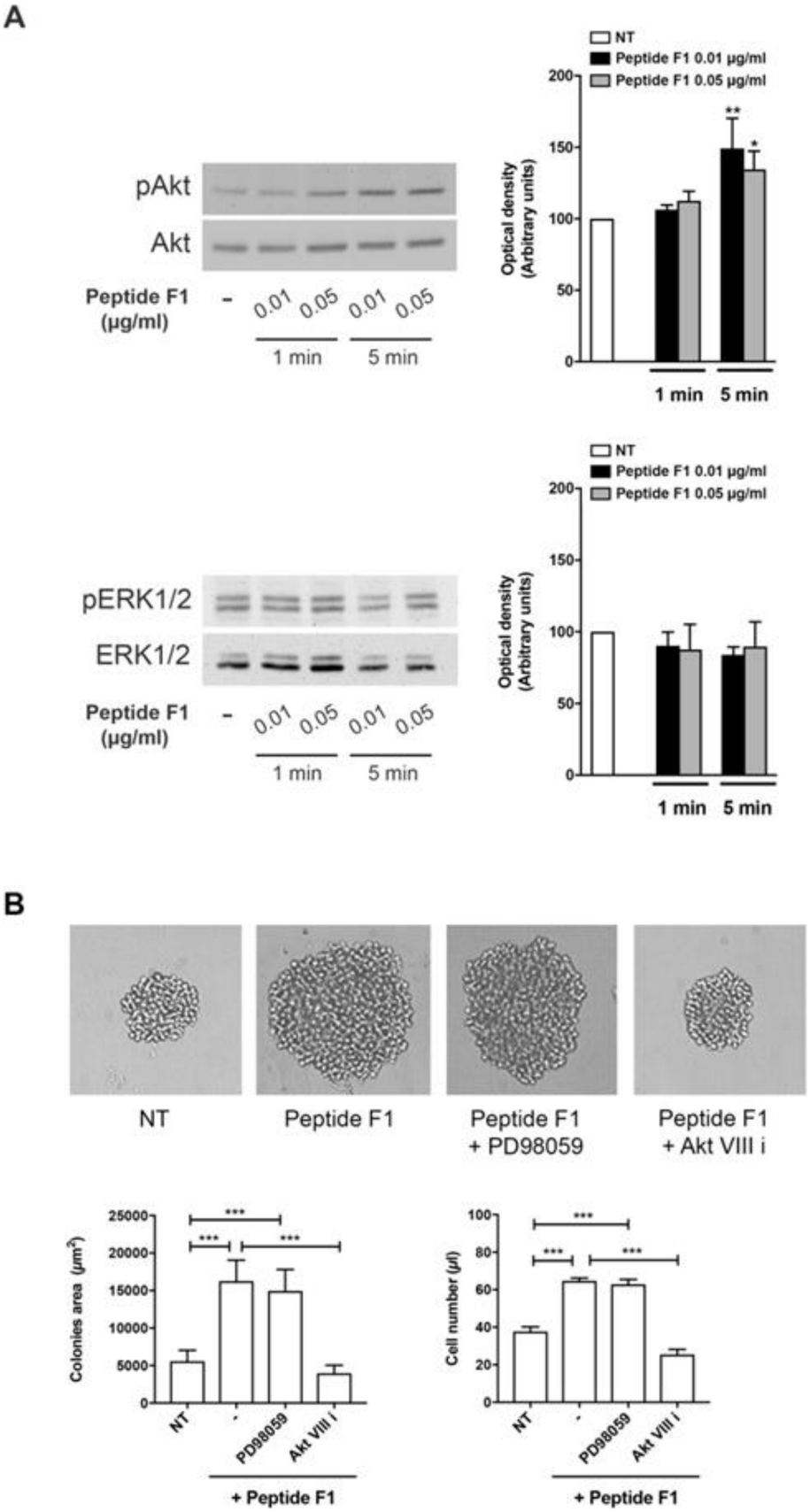
A
pAkt
Akt
Peptide F1 (µg/ml)
-
0.01
0.05
0.01
0.05
1 min
5 min
NT
Peptide F1 0.01 µg/ml
Peptide F1 0.05 µg/ml
Optical density (Arbitrary units)
200
150
100
50
0
**
*
1 min
5 min
pERK1/2
ERK1/2
Peptide F1 (µg/ml)
-
0.01
0.05
0.01
0.05
1 min
5 min
NT
Peptide F1 0.01 µg/ml
Peptide F1 0.05 µg/ml
Optical density (Arbitrary units)
200
150
100
50
0
1 min
5 min
B
NT
Peptide F1
Peptide F1 + PD98059
Peptide F1 + Akt VIII i
Colonies area (µm²)
25000
20000
15000
10000
5000
0
***
***
***
NT
-
PD98059
Akt VIII i
+ Peptide F1
Cell number (µl)
100
80
60
40
20
0
***
***
***
NT
-
PD98059
Akt VIII i
+ Peptide F1

Figure 7

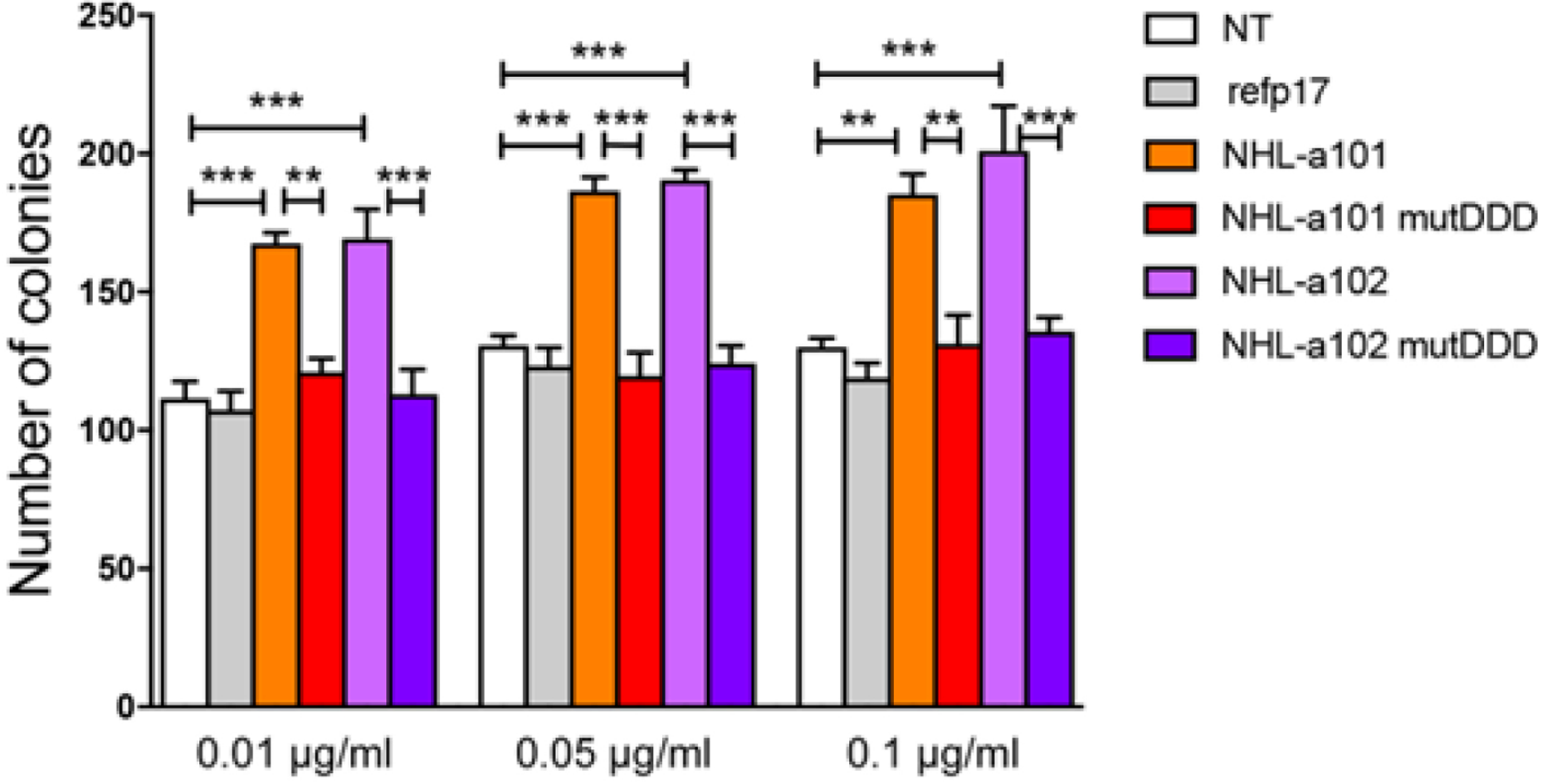
Number of colonies
250
200
150
100
50
0
0.01 µg/ml
0.05 µg/ml
0.1 µg/ml
***
**
NT
refp17
NHL-a101
NHL-a101 mutDDD
NHL-a102
NHL-a102 mutDDD

Figure 8